

LIGHTCURVE SIGNATURES OF MULTIPLE OBJECT SYSTEMS IN MUTUAL ORBITS

Eileen V. Ryan and William H. Ryan

*Magdalena Ridge Observatory, New Mexico Institute of Mining and Technology
801 Leroy Place, Socorro, NM 87801*

1. INTRODUCTION

The lightcurves of objects in mutual orbits will display occultation and/or eclipse events, collectively referred to as ‘mutual events’, under favorable geometric circumstances. Given that the unresolved image of a multiple object system is simply the sum of the scattered light from each individual object, these mutual events will appear as attenuations in the total detected light when one object (resulting in an occultation) or its shadow (resulting in an eclipse) passes in front of the other. Under certain geometric circumstances, it is possible to have both types of events occurring simultaneously, resulting in an even deeper minimum of the observed lightcurve.

The technique of using the observation of anomalous attenuations in minor planet lightcurves to identify binary systems has proven to be very fruitful. However, recently, there has been interest in identifying potentially hostile companions to artificial satellites. However, these companions will typically be much smaller relative to the parent body than previously observed asteroid binary systems, and hence, the expected attenuations due to the mutual events will be rather modest. Therefore, in the next two sections, we briefly review how this method has been used to identify minor planet binary systems in general, and then discuss the detection limits of this technique as applied to resident space objects.

2. IDENTIFICATION OF BINARY MINOR PLANET SYSTEMS

The identification of mutual event signatures in the lightcurves of asteroids has led to the detection of several asynchronous Near Earth Asteroid [1] and Main Belt [2, 3,4] binary systems. Such asynchronous systems, where the rotation period of the primary object differs from the mutual orbital period of the system, usually display the most unambiguous signature of a binary system. In particular, Fig. 1 shows lightcurve attenuations observed in the binary system 3782 Celle. In this figure, the light variation due to the 3.84 hour rotational period of the primary object has already been subtracted out in order to isolate the attenuations resulting from the 36.6 hour orbital motion of the two companions.

A schematic illustrating the origin of these attenuation features is shown in Fig. 2. For clarity, the objects are both assumed to be spherical and of equal albedo. In this figure, the top panel shows a smaller secondary object revolving (clockwise as viewed from above) around a larger primary object at zero solar phase angle. The resulting lightcurve, which is obtained by summing of the scattered light from both targets and then converting to magnitude units, is shown in the bottom panel.

Suspected binary systems where the primary’s rotational period and the mutual orbit’s period are synchronous have also been observed [5]. However, the binary nature of these systems is more difficult to confirm since the signatures of the mutual events appear simply as more extended depressions in the minima already resulting from the asteroid’s rotation.

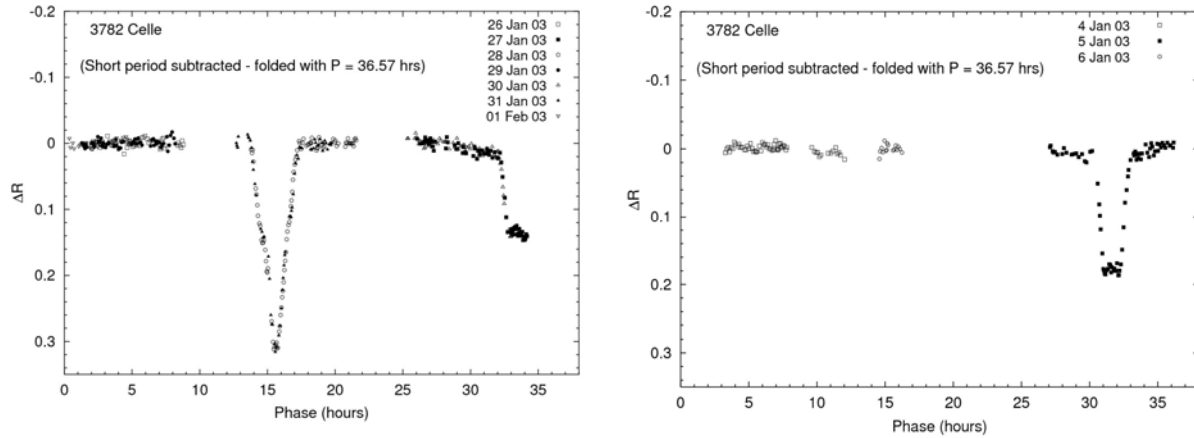


Fig.1. Short-period subtracted lightcurves of the minor planet binary system 3782 Celle as the two asteroids occult each other. The secondary/primary diameter ratio is 0.43 ± 0.01 (with the primary body having a diameter of about 6 km, and located in the main asteroid belt). The primary's rotational period is 3.84 hours, and the orbital period of the system is 36.57 ± 0.03 hours.

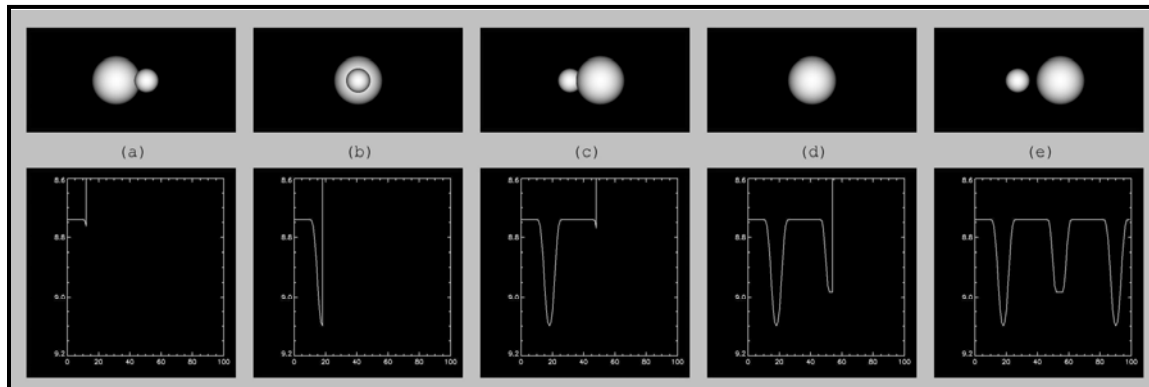


Fig. 2. Schematic illustrating the origin of the observed attenuations in binary systems. The smaller secondary object is revolving clockwise as viewed from above. The vertical axis is in units of magnitudes and the horizontal axis represents arbitrary rotational phase. Event (a) shows the onset of a primary occultation (i.e., secondary occulting the primary) with the full occultation observed in (b). Events (c) and (d) display the same for a secondary occultation (i.e., secondary occulting the primary). Event (e) simply shows the combined light when no attenuations are occurring.

3. APPLICATION TO ARTIFICIAL TARGETS

To determine the feasibility of detecting co-orbiting satellite systems via lightcurve attenuations, it must be recognized that the secondary will typically be much smaller relative to the parent body than previously observed asteroid binary systems, and hence, the expected attenuations due to the mutual events will be rather modest. In Fig. 3a, we examine the predicted maximum attenuation (in units of magnitude) for a primary occultation as a function of the relative size of the targets for two different scattering models at zero phase angle. The geometric scattering model results in a lightcurve that is simply the observed geometric total cross section of the two objects in the various configurations depicted in the top panel of Fig. 2. Geometric scattering can be used to model the shapes of asteroids observed near opposition at low phase angles since, under these circumstances, it approximates the

Lommel-Seeliger scattering model that is frequently used to model asteroid surfaces. However, this may be less applicable to artificial targets. Therefore, the attenuation results using a Lambertian model, which is more applicable to painted surfaces, are also plotted.

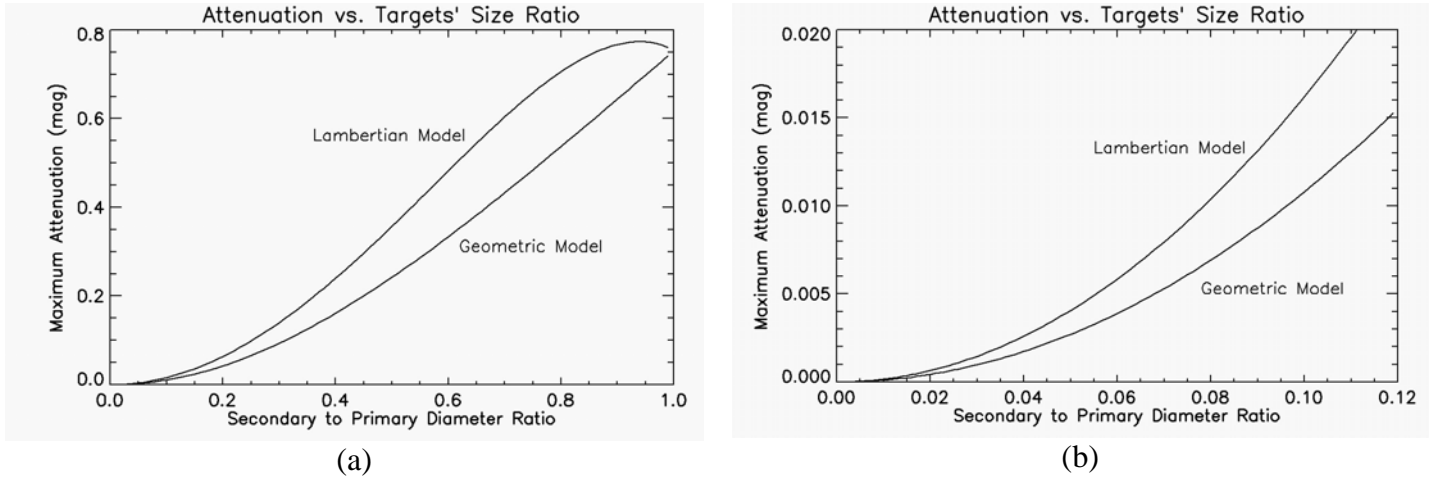


Fig. 3. The left-hand figure plots the predicted lightcurve maximum attenuations as a function of the components' size ratio for both a simple geometric and a Lambertian scattering model. Note that this attenuation is in addition to any lightcurve features resulting from the shapes of the individual objects. The right-hand figure shows the same plot, but with the scale chosen to illustrate the secondary component detection limits for systems capable of 1% and 0.1% photometry.

In Fig. 3b, the maximum attenuation versus component size ratio relationship is scaled to elucidate the detection limits associate with 1% (0.01 magnitude) photometry, which is the canonical standard of 'good' photometry, and 0.1% (0.001 magnitude) photometry, which is the goal of high precision photometry. Note that for the geometric scattering model, 1% photometric precision corresponds to a component size ratio of $D_s/D_p \sim 0.1$ and 0.1% precision corresponds to $D_s/D_p \sim 0.03$; with the Lambertian model, precision limits correspond to slightly smaller size ratios. These results may be interpreted as "1-sigma" detection limits for a single data point. However, an attenuation event will usually be recorded by many lightcurve points, which significantly increases the confidence factor. Another important consideration is that these model results are for spherical components. Therefore, if either of the individual components generate a non-trivial lightcurve, considerably higher photometric precision would be required in the raw data to reach these detection limits since the light variations due to the individual components must first be subtracted out. In Fig. 4, we compare these detection limits to the predicted signal to noise performance as a function of the target's magnitude for both a 0.35-meter portable telescope and the Magdalena Ridge Observatory (MRO) 2.4-meter telescope facility scheduled to come online in late Fall 2006. These results assume 10 second exposures and few arc-second seeing conditions for the 0.35-meter (typically deployed at low elevations), and arc-second seeing for the mountaintop location (the elevation is 10,612 feet) of the 2.4-meter. As can be seen in the figure, the magnitude limit (dominated by the primary satellite) of a secondary satellite of approximately one tenth the size of the primary is on the order of visual magnitude $V=13$ for the 0.35-meter, and $V=18$ for the 2.4-meter telescopes.

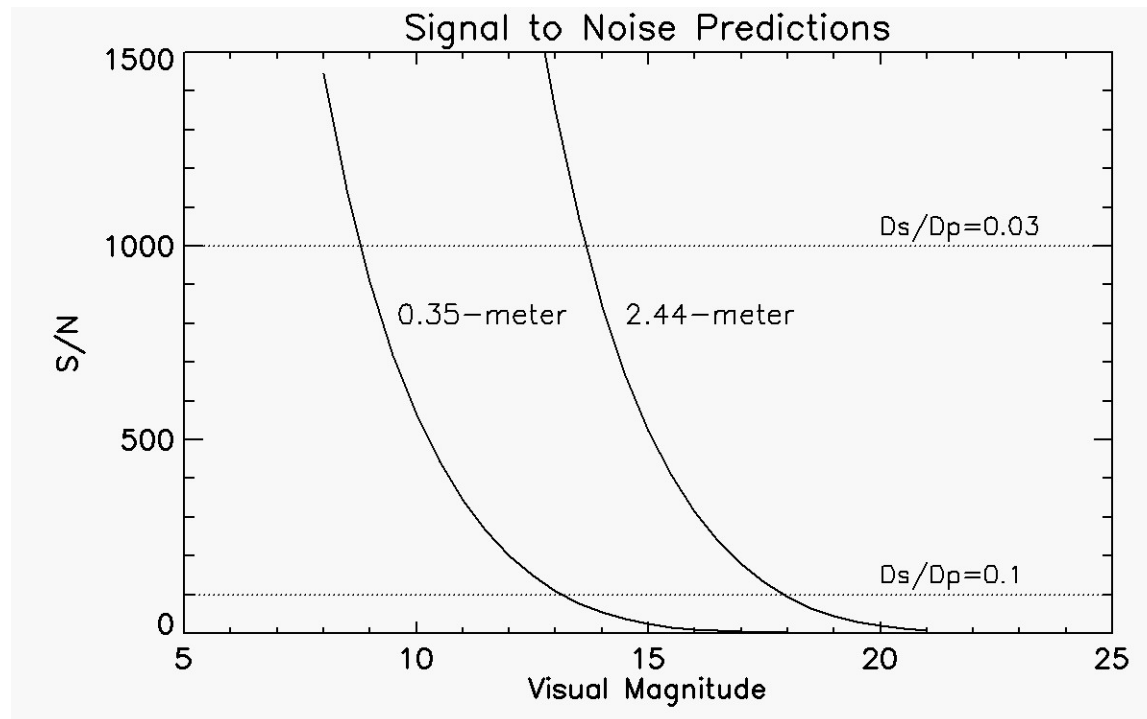


Fig. 4. Photometric signal to noise predictions as a function of magnitude for a 10 second exposure using the MRO 2.4-meter telescope and a portable 0.35-meter imaging system. For reference, the horizontal lines corresponding to the 1% and 0.1% photometry limits are plotted, along with their associated typical target size ratios (D_s/D_p) from Fig. 3.

4. CONCLUSION

The preceding calculations indicate that it is possible that the same lightcurve techniques used to identify minor planet binary systems can be used to detect maneuvering nano- and micro-satellite companions to artificial resident space objects with dimensions of one to a few meters. However, the ability to accomplish this would require favorable geometric circumstances, in particular, a relative orientation that would lead to occultation or eclipse events. It also would require knowledge of a well determined lightcurve for the primary satellite in the absence of attenuation events.

5. REFERENCES

1. Pravec et al. (2006). Photometric survey of near-Earth binary asteroids, *Icarus* 181, 63-93.
2. Ryan, W.H., E.V. Ryan, and C. Martinez (2004). 3782 Celle: Discovery of a Binary System within the Vesta Family of Asteroids. *Planetary and Space Science*, 52, 1093 -1101.
3. Warner et al. (2005), (5905) Johnson, IAU Circular 8511 and (76818) 200 RG79, IAU Circular 8592.
4. Krugly et al. (2005). Binary main-belt asteroid 11264 Claudiomaccone, presented at *Dynamics and Physics of Solar System Bodies*, May 22-25, 2005, Kiev, Ukraine.
5. Behrend et al. (2004). (854) Frostia, IAU Circular 8389, (1089) Tama, IAU Circular 8265, (1313) Berna, IAU Circular 8292, and (4492) Debussy, IAU Circular 8354.